Thus, only local crystal field perturbations which lower the symmetry will have an effect on the separation between the levels of the doublet and/or the transition probability. In other words, hydrostatic pressure will have no effect on the line shape to second order. Thus, small perturbations on the local crystal field symmetry are directly manifest in terms of the effects on the absorption line shape.

IV. CONCLUSION

The model presented here offers a means for studying the effect of intrinsic and induced perturbations on the local crystal field symmetry for transitions within a non-Kramers doublet for the three cases of local crystal-field symmetry considered. Using uniaxial stress, the spin-lattice coupling parameters can be evaluated independently of the concentration of the impurity ion to the extent that the impurity concentration is not so large as to affect the shape of the absorption line.

The model is applicable to a variety of systems, among them are MgO: Fe^{2+}, [12] Al_2O_3: Fe^{2+}, [9] and CaF_2: U^{4+}. [13,14] For the latter system, the model has been compared quite favorably with the results of uniaxial strain measurements. [14]

ACKNOWLEDGMENTS

The authors wish to express thanks to J. D. Stettler and E. R. Wilkinson of this Laboratory for useful discussions.

[1]G. Watkins and E. R. Feher, Bull. Am. Phys. Soc. 7, 29 (1962).
[2]E. R. Feher, Phys. Rev. 136, 145 (1964).
[3]C. M. Bowden, H. C. Meyer, and P. L. Donoho, Inter. J. Quantum Chem. Suppl. 3, 617 (1970).
[3a]*Note added in proof.* The term doublet is used here to denote the $|\Delta M_S| = 2$ transition within a ground triplet.
[4]J. W. Culvahouse, D. P. Schinke, and D. L. Foster, Phys. Rev. Letters 18, 117 (1967).
[5]C. M. Bowden, H. C. Meyer, and P. L. Donoho, preceding paper, Phys. Rev. B 3, xxx (1971).
[6]K. A. Mueller, Phys. Rev. 171, 350 (1968).
[7]W. Voigt, *Lehrbuch der Kristallphisik* (Teubner, Leipzig, 1910).
[8]N. Bloembergen, Science 133, 1363 (1961).
[9]C. M. Bowden, H. C. Meyer, and P. L. Donoho, Inter. J. Quantum Chem. Suppl. 4, 1971 (1970).
[10]J. S. Gradshtegn and J. M. Ryzhik, *Table of Integrals, Series and Products* (Academic, New York, 1965).
[11]H. B. Huntington, *Solid State Physics* (Academic, New York, 1958), Vol. 7, p. 276.
[12]D. H. McMahon, Phys. Rev. 134A, 128 (1964).
[13]P. K. Wunsch, P. L. Donoho, H. C. Meyer, and C. M. Bowden, Bull. Am. Phys. Soc. 15, 250 (1970).
[14]P. L. Donoho, P. K. Wunsch, P. F. McDonald, C. M. Bowden, and H. C. Meyer, Bull. Am. Phys. Soc. 15, 250 (1970).

PHYSICAL REVIEW B VOLUME 3, NUMBER 3 1 FEBRUARY 1971

Conduction-Electron Spin Resonance in a Lithium Film*

Joe H. Pifer and Richard Magno
Rutgers University, New Brunswick, New Jersey 08903
(Received 2 October 1969)

The use of a linear resonator instead of a microwave resonant cavity increases the sensitivity of any resonance spectrometer when studying electron resonance in metals. This technique is used to study the temperature dependence of the line shape of the conduction-electron spin resonance in a lithium film for thicknesses ranging from 0.3 to 30 skin depths. Dyson's theory is found to apply at high temperatures. Deviations below 120 °K due to the anomalous skin effect provide a method of determining the microwave surface impedance in the alkali metals.

I. INTRODUCTION

In this paper we discuss a simple modification of the conventional electron-spin-resonance (ESR) technique for metals, which results in a sensitivity gain of five times. We then use this technique to verify Dyson's[1] theory of the conduction-electron spin resonance (CESR) line shape in lithium films whose thicknesses range from 0.3 to 30 skin depths. Dyson's theory has previously been verified[2] for thick samples and for dispersions or powders whose grain size is small compared to the skin depth. Here we study a *single* film of uniform thickness. Data were taken from 4.2 °K to room temperature. At low temperatures, the anomalous skin effect is found to modify the line shape in an extremely simple manner.

The usual reflection technique for studying CESR in metals is to place the sample in a cavity which is critically coupled to one arm of a microwave bridge.

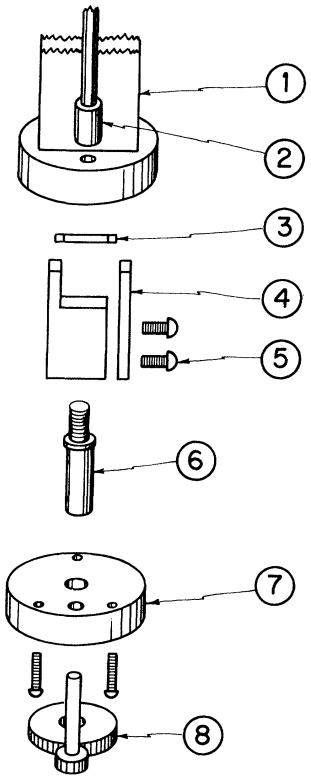

FIG. 1. Experimental setup for mounting the sample in the waveguide: (1) waveguide, (2) coupling rod, (3) cylindrical quartz substrate with lithium film, (4) Teflon sample holder, (5) nylon screw, (6) rotation shaft, (7) baseplate, and (8) gears.

The modification we use is as follows: The sample, in the form of a straight wire or film one-half wavelength long, is suspended in a shorted waveguide. No resonant cavity is needed since the sample itself forms a resonant structure (a half-wave dipole). By proper orientation in the waveguide, the resonator can be critically coupled to the guide. Thus the resonator is electrically identical to a resonant cavity and can be used in a conventional ESR spectrometer. It could equally well replace a transmission cavity.

Resonant coils are routinely used in nuclear magnetic resonance (NMR) and have previously been used to detect ESR in insulators at X band[3] and lower frequencies.[4] In the present case where the resonator is the sample, there is no need to deform it into a coil. Pippard[5] has used a coaxial linear resonator at microwave and lower frequencies to measure the nonresonant surface impedance in metals.

In Sec. II we give the details of the linear resonator, its construction and its sensitivity as compared to conventional cavities. In Sec. III we give a slight extension of Dyson's theory of the line shape to the case of arbitrary rf excitation of the two faces of the sample and discuss several limiting cases including the modification produced by the anomalous skin effect. In Sec. IV we compare the theory and experiment.

II. EXPERIMENTAL DETAILS

A. Linear Resonator

Figure 1 shows the arrangement used to hold the sample in the waveguide and orient it for critical coupling. When the sample is exactly parallel to the broad face of the waveguide, perpendicular to the electric field, no coupling occurs. As the sample is rotated in either direction, the component of the electric field along the wire excites currents in the wire. Critical coupling occurs at $\approx \pm 5^\circ$ depending upon the Q of the resonator. When resonating, the electric field lines at the surface of the sample are along the wire and the magnetic field lines are circles around the wire. With this arrangement the rf field is intense near the sample and weak at the waveguide so that essentially all the power is absorbed by the sample and there is a gain in sensitivity over having put the sample in a conventional cavity. The maximum ESR signal is seen when the external magnetic field is parallel to the wire axis. When the field is perpendicular, the signal is reduced by one-half. The frequency of the resonator is determined by its length: A film 1.04 cm long on a quartz capillary tube 1.5 mm in diam held in a Teflon sample holder has a resonant frequency around 9.0 GHz. The walls of the waveguide and the sample holder have only a slight effect upon the Q of the resonator. A lithium film at room temperature typically has a Q of 900. The arrangement shown gives a very stable noise-free balance down to liquid-helium temperatures. Severe microphonic noise occurs if the sample is not held firmly by the sample holder.

In wire samples where damage to the sample is not a concern, a simpler sample holder made of $\frac{1}{4}$-in. Teflon rod with a hold drilled through it can be used. Modulation pickup sometimes occurs with this holder when the sample is held tightly by the Teflon, but disappears when the hole is enlarged and the sample is secured with vacuum grease. A tapered $\frac{3}{16}$-in. brass rod also works as a holder. The most trouble free holder for wires was found to be a Styrofoam block. In all cases considerable care is required in alignment to prevent poor Q or a shift in the resonant frequency with coupling. Careful attention to cleanliness is also necessary due to the sensitivity. A Teflon sample holder can be adequately cleaned by boiling for 5 min in concentrated NaOH, followed by a thorough rinsing and boiling in de-ionized water. In the lithium films no unwanted resonances were observed, but high-purity silver and copper wires frequently had spurious resonances presumably due to surface oxide or hydroxide layers.

B. Sensitivity

In order to compare the sensitivity of the linear resonator with the conventional resonant cavity, a resonator was made by drawing molten Li into a capillary tube and cutting it to a one-half wavelength. After recording the CESR signal at room temperature, the sample was cut in half to make it nonresonant and placed on the bottom of a silver-plated half-wave cavity operating at the same frequency as the resonator and the signal recorded under identical experimental conditions. The signals (see Fig. 2) show that the linear resonator increases the sensitivity by a factor of about 5. In order to check that the proximity of the walls did not affect the signal in the half-wave cavity, the sample was also placed at the center of a full-wave cavity. The resonator signal was better by ten times as expected since the surface of the full-wave cavity is twice that of the half-wave cavity.

This gain in sensitivity may be understood by considering what happens to the power incident on a microwave cavity. The power goes into Joule heating of the cavity walls, heating of the sample, and resonance absorption by the sample. The resonance absorption, which is proportional to the electron susceptibility, is very small compared to the Joule heating. Dyson has shown it can be written as the Joule heating of the sample times some resonant terms. Then to have an optimum resonance signal it is necessary to have most of the incident power dissipated in the sample and not in the cavity walls. Thus some experimenters place the sample in a cavity wall. Ideally, the entire cavity should be made of the sample material. We have done the equivalent thing by making the sample a resonant structure. To evaluate the theoretical gain in sensitivity we have integrated the Poynting flux over the area of the walls of the half-wave cavity and over the sample and find that $\approx \frac{1}{10}$ of the incident power is dissipated by the sample. Thus, if all the power is dissipated in the resonator, a gain of about ten would be expected. We observe a gain of five.

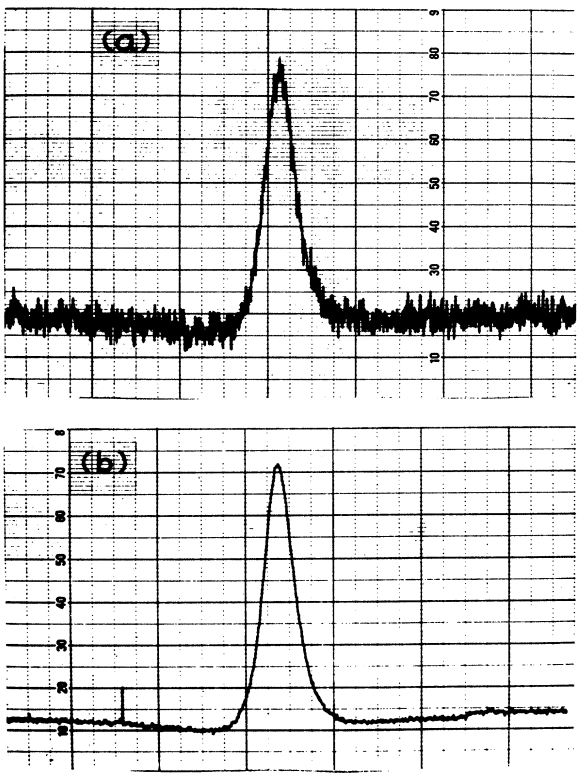

FIG. 2. Comparison of the derivative of the CESR power absorbed by a lithium rod 1.1 cm long, 1.0 mm in diam, when (a) placed in a half-wave cavity and (b) used as a linear resonator under identical experimental conditions: 4.5×10^{-6} W of microwave power, modulation 0.06 G peak to peak at 100 cps, 0.1-sec lock-in time constant, room temperature. The lock-in gain for (a) is five times the gain for (b).

C. Sample Preparation and Experimental Procedure

The starting material for the films was 99.97% lithium.[6] An electron beam was used to evaporate the material from a molybdenum boat. The lithium was first bombarded until it melted and the nitride coating broke down leaving a shiny surface. This step also coated the bell jar with lithium, which acted as a getter to improve the starting vacuum of less than 1×10^{-6} Torr. A shutter was then moved and the sample was evaporated rapidly to obtain a mirror surface. With 160 W of electron beam power, a deposition rate of 0.6 μ/sec on a flat plate could be achieved. However, the narrowest CESR lines, indicating the purest samples, were obtained with a somewhat slower rate. The substrate was a 1.5-mm-diam quartz capillary tube located 10 cm above the boat and rotated at 120 rpm. A second film to be used for measuring the thickness and resistivity was evaporated at the same time on a Pyrex plate located within 1 cm of the rotating rod. Copper electrodes were evaporated in a prior pumpdown. The flat film should be π times thicker than the cylindrical film.

After evaporation the films were carried in a dry helium atmosphere to a dry box. Lithium does not react with dry air and films could be stored in the dry box for up to a week without any change in appearance or resonance properties. Lithium does react with quartz and Pyrex if the temperature is raised much above room temperature. We had some trouble with substrate heating and reaction at very high evaporation rates.

After the cylindrical film was mounted, the ESR probe was evacuated, then filled with helium gas. The line shape was recorded on a chart recorder using a conventional homodyne spectrometer. A 200-cps magnetic field modulation was used. In or-

der to get more accurate values of the A/B ratio, the following procedure was used. A baseline was first established by moving 100 G below the resonance. Then several sweeps were made through the peak followed by sweeps through the minimum and then the peak again. Finally the baseline was measured above resonance. A/B was determined by measurement with dividers and a scale. The temperature was stabilized to within $\frac{1}{2}$ °K during the measurement.

Considerable care was devoted to checking that the line shape was independent of the manner in which the spectrometer was balanced or arranged. For operation with the klystron frequency locked to the sample cavity, it was found that the only factor that gave spurious line shapes was the presence of reflections in the bridge. When these were eliminated by removing all bends in the sample arm of the bridge, it was very difficult to adjust the spectrometer to give a spurious line shape. Different shaped sample holders which held the sample at various distances from the shortened end of the waveguide, temperature cycling, and storage of the sample for several days had no effect. The modulation amplitude was varied to ensure that it had no effect on the line shape.

In order to measure the thickness and resistivity, the flat film was mounted in a four-lead resistance probe and the resistance was measured as a function of temperature using a lock-in amplifier operating at 20 cps. The temperature in both cases was measured by a copper-constantan thermocouple calibrated by a platinum resistance thermometer. The data were generally taken as the samples were slowly cooled for the first time.

An attempt to measure the thickness more accurately than with the resistance technique was made by using an ac bridge to measure the change in resistance of a known volume of distilled water when the lithium sample was reacted with it. The technique easily had enough sensitivity to measure our thinnest film to 1%. However, the resistance of the cell drifted rapidly upward, indicating a loss of conducting ions. The loss was probably due to reaction of the lithium with dissolved gases such as carbon dioxide. The flat films were too thick to use the optical interference method. In very thick films we found that titration was accurate to 10%.

III. THEORETICAL LINE SHAPE

A. General Case

The experimentally measured quantity is the derivative with respect to field of the power absorbed by the sample as the magnetic field is swept through resonance. Since the power is given by the Poynting flux into the sample, Maxwell's equations must be solved for the rf fields at the surface, subject to the boundary conditions imposed by the sample. This is more complicated than the usual skin-depth calculation since the spin-relaxation time T_2 can be much longer than the orbital collision time τ. Thus as the electron diffuses away from the surface, the coherent precession of the spin produces a rf field far beyond the skin-depth region. The fields in the metal are then a linear combination of damped waves described by the propagation constants[1,7]

$$k_1^2 = 2i/\delta^2 , \tag{1}$$

$$k_2^2 = 2(1+ix)/\delta_e^2 , \tag{2}$$

where $\delta = (c^2\rho/2\pi\omega)^{1/2}$ is the classical skin depth and $\delta_e = (2DT_2)^{1/2}$ is the spin depth – the distance perpendicular to the surface that a spin can diffuse in one relaxation time. D is the diffusion constant. $x = (\omega - \omega_0)T_2$ is a dimensionless variable giving the distance the magnetic field $H_0 = \omega_0/\gamma$ is from the resonant field $H = \omega/\gamma$. $\omega/2\pi$ is the microwave frequency and ρ is the electrical resistivity.

Dyson[1] has solved for the power absorbed by a large plate of arbitrary thickness with the external field perpendicular to the face and a linearly polarized rf field H_1 parallel to it. The calculation is complicated because the relation between the magnetization M and H_1 is nonlocal due to the diffusion of the electrons. Dyson solved for M by expressing it as an integral of a Green's function over the diffusion and relaxation probabilities. Kaplan[7] pointed out that the problem could be solved much more simply by assuming that M is described phenomenologically by a Bloch equation as modified for diffusion by Torrey.[8]

Dyson's calculation applies to a flat plate. Here the experimental configuration is a cylindrical rod with H_0 perpendicular to its axis and a coaxial rf field. Since δ and the film thickness are small compared to the radius of the cylinder, it is a good approximation to replace the cylinder with a flat plate. Further, since it is experimentally observed[9,10] that the line shape does not depend on the orientation of H_0, we take H_0 perpendicular to the plate. Thus Dyson's result would apply except that the boundary conditions are different. He assumed that H_1 is the same on both faces of the plate. For a linear resonator the rf field at the inside surface is nearly zero. This is easily seen by placing an Amperian loop at the inner surface, coaxial with the cylinder. Since the current through the loop is zero, H_1 is zero except for a negligible contribution from the displacement current. Using Kaplan's method we have solved for the CESR line shape of a flat plate when the rf field is equal to H_1 on one face and $-bH_1$ on the other, where b is arbitrary. When comparing with experiment[11] we take $b = 0$. Lampe and Platzman[10] have used Dyson's technique to solve for the line shape in a plate where $d \gg \delta$ and $\delta_e \gg \delta$ subject

to these same boundary conditions.

We find that the power absorbed by the sample is

$$P = (c/4\pi)^2 H_1^2 \,\mathrm{Re}(Z), \tag{3}$$

where H_1 is the amplitude of the circularly polarized rf magnetic field at the surface of the plate. A linearly polarized field can be broken up into two counter-rotating circularly polarized parts. The component rotating in the antiresonant sense gives negligible field dependence and is neglected. The surface impedance Z to first order in the electron susceptibility χ_0 is given by

$$Z = (\rho/d)\,[F + (\pi\omega_0 T_2 \chi_0\, d^2/\delta_e^2)\, G]\ , \tag{4}$$

with

$$F = (1+b)^2\, u\cot u - (1-b)^2\, u\tan u\,, \tag{5}$$

$$\begin{aligned} G = -\,i(u^2-w^2)^{-2}\{&(1+b)^2\,u^2\cot^2 u\,[(u^2-w^2)\sec^2 u \\ &-(3u^2-w^2)\,u^{-1}\tan u + 2u^2\,w^{-1}\tan w] \\ &+(1-b)^2\,u^2\tan^2 u\,[(u^2-w^2)\csc^2 u \\ &+(3u^2-w^2)\,u^{-1}\cot u - 2u^2\,w^{-1}\cot w]\}, \end{aligned} \tag{6}$$

where d is the sample thickness and

$$u = (1+i)d/2\delta, \tag{7}$$

$$w = (\xi + i\eta)d/2\delta_e\,, \tag{8}$$

where

$$\eta = [(1+x^2)^{1/2}+1]^{1/2}, \tag{9}$$

$$\xi = (\mathrm{sgn}x)\,[(1+x^2)^{1/2}-1]^{1/2}\,. \tag{10}$$

When $b=-1$, Z reduces to Dyson's expression.

B. Line Shape for Thin Films

Equation (4) is a general result for arbitrary values of the parameters and is unnecessarily complicated for most applications. In fairly pure metals $\delta_e \gg \delta$, e.g., in lithium at room temperature $\delta_e/\delta \approx 10$. If we are interested in films for which d is comparable to δ, then $d/\delta_e \ll 1$. Keeping only the lowest-order term in d/δ_e in Eq. (4) and dropping the term independent of χ_0, we find

$$P = \left(\frac{c}{4\pi}\right)^2 H_1^2\,\mathrm{Re}\left(\frac{2\pi\rho\omega_0 T_2\chi_0 d}{\delta_e^2}\;\; i(1-b)^2\,\frac{\tan^2 u}{w^2}\right). \tag{11}$$

This approximation, which is equivalent to assuming that the magnetization is uniform across the sample, is very good since the next-order term vanishes when the derivative is taken. Taking the real part and differentiating,

$$\begin{aligned} \frac{dP}{dH_0} = -\left(\frac{c}{4\pi}\right)^2 H_1^2\,\frac{4\pi\rho\omega_0\chi_0 T_2}{d}\;(1-b)^2 \\ \times\left[\kappa\frac{d}{dx}\left(\frac{1}{1+x^2}\right)+\nu\frac{d}{dx}\left(\frac{x}{1+x^2}\right)\right], \end{aligned} \tag{12}$$

where

$$\kappa = \frac{2\sin\lambda\sinh\lambda}{(\cosh\lambda+\cos\lambda)^2}\,, \tag{13}$$

$$\nu = \frac{\sin^2\lambda - \sinh^2\lambda}{(\cosh\lambda+\cos\lambda)^2}\,, \tag{14}$$

and $\lambda \equiv d/\delta$. We have ignored a term coming from the nonresonant variation of ω_0 since it is smaller than the resonant terms by a factor $\Delta H/H_0$, where ΔH is the width of the resonance. The line shape is a mixture of the derivatives of the absorptive and dispersive parts of a Lorentzian line. The Lorentzian line shape is not surprising since it is known to be the solution of the Bloch equation; nuclei diffusing in a liquid give a Lorentzian NMR signal. The mixture occurs since the phase of the rf field changes as it propagates into the metal. Then when the phase-sensitive detector is set to detect the absorption of electrons at the surface, it will detect a mixture of absorption and dispersion by electrons at greater depths. Notice that only the $(1-b)^2$ term contributes; the line shape for thin films is the same for one-sided as for symmetric excitation. This is easily understood since for antisymmetric excitation, $b=1$, H_1 varies as $\sinh k_1 z$ which is zero at the center of the film, while for $b=-1$, H_1 varies as $\cosh k_1 z$ and remains large across the film.

For small λ, $\kappa \approx \frac{1}{2}\lambda^2$ and $\nu = \frac{1}{6}\lambda^4$, while for large λ, $\kappa \approx 0$ and $\nu \approx 1$. Thus for very thin films the line shape is totally absorptive, while for very thick ones it is dispersive. Note that at $\lambda = \pi$, κ passes through zero. For $0 < \lambda < \pi$ the two signals add together so that the peak in the signal is on the low-field side and the minimum is on the high-field side of the resonant field as shown in Fig. 3. For $\pi < \lambda < 2\pi$ the situation is reversed. Another reversal would occur at 2π except κ is so small it cannot be observed. Thus the maximum occurs on the high-field side of

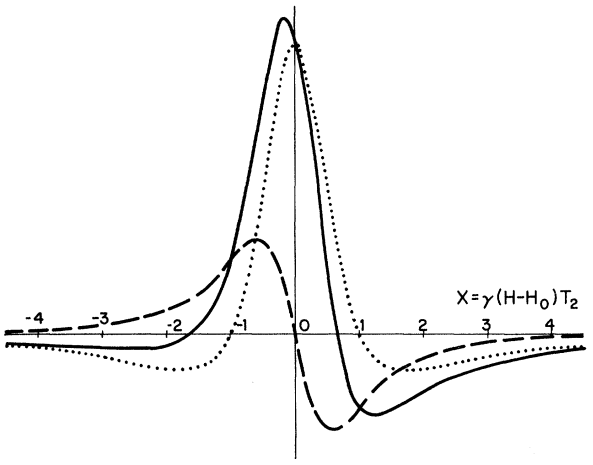

FIG. 3. Superposition of the derivative of a Lorentzian absorption curve (dashed) and a dispersion curve (dotted) to give a typical thin-film CESR line shape (solid).

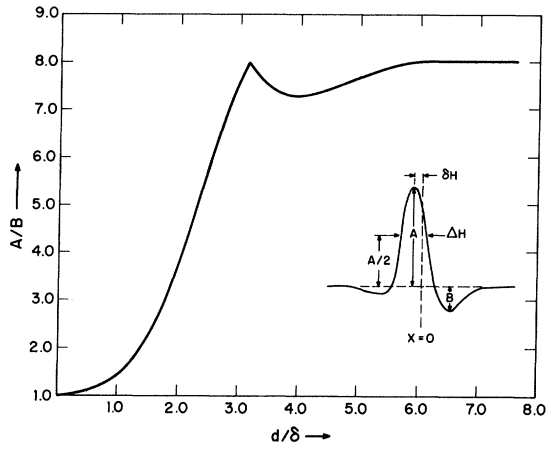

FIG. 4. Theoretical A/B vs d/δ for the derivative of the CESR power absorption in samples where $\delta/\delta_e \ll 1$. The insert defines A and B on a typical CESR line.

resonance only in the range $\pi < \lambda < 2\pi$. Note that when $\lambda = \pi$, the phase of the eddy current flowing in the skin region has been shifted by π.

A frequently used and very sensitive measure of the line shape is the A/B ratio, that is, the ratio of the maximum peak to the minimum peak.[12] For a Lorentzian absorption, $A/B = 1.0$, while for dispersion $A/B = 8.0$. The theoretical plot of A/B vs λ is shown in Fig. 4. Accompanying the rise in the A/B ratio is a shift in the position of the resonant field from the zero crossing between the peaks to the center of the maximum peak and a decrease in the linewidth. These quantities are shown as solid lines in Figs. 5 and 6. The definitions are shown in the insert to Fig. 4.

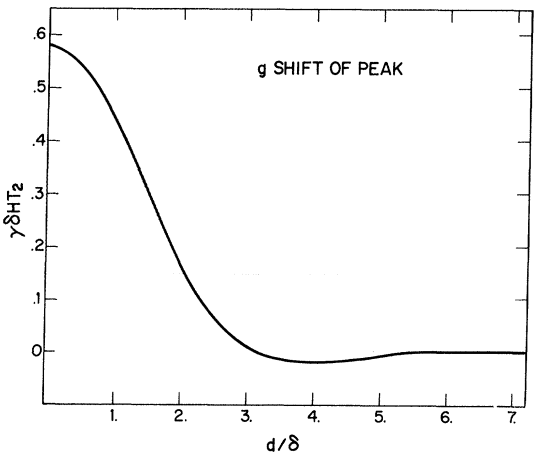

FIG. 5. Theoretical shift from the resonant field of the peak of the derivative of the CESR power absorption vs d/δ for samples where $\delta/\delta_e \ll 1$. The shift δH is expressed in units of $1/\gamma T_2$ and is defined by the insert in Fig. 4.

C. Line Shape for Thicker Films

In Sec. III B we found for $d/\delta_e \ll 1$ that the CESR line shape made a dramatic change when $\lambda \equiv d/\delta$ went from 0 to π due to the phase change in the skin (k_1) currents. The simple picture breaks down for thicker samples where d is large or for very dirty samples where impurity spin scattering reduces δ_e. We expect additional changes when the phase of the spin (k_2) currents goes from 0 to π. But the effect of the k_2 currents may be considerably different since by Eqs. (1) and (2) k_2 depends resonantly upon the magnetic field but k_1 does not. For thick clean films where $\delta/\delta_e \ll 1$, our previous discussion indicates that the line should be a Lorentzian dispersion line with $A/B = 8.0$ independent of d. The variation due to d/δ_e should then appear superimposed on this plateau. The two variations are not nicely separated for dirty samples where $\delta \approx \delta_e$.

Rather than consider additional approximations to Eq. (4), we have programmed the entire expression and numerically calculated the line shape.[13,14] Figure 7 shows the theoretical A/B ratio vs λ for several values of δ/δ_e. Note that in each case A/B rises from 8.0 to a maximum, then drops to another higher plateau.[15] Once the second plateau has been reached, the line shape is independent of sample thickness. Feher and Kip[2] have previously calculated this plateau value for various δ/δ_e and have made a comparison with experiment. Note that in curves A, B, and D where $b = 0$, the peak occurs not at π but at $d/\delta_e = 1.35 < \frac{1}{2}\pi$, while in C where $b = -1$, $d/\delta_e = 2.70 < \pi$. As anticipated the variation of k_2 with magnetic field shifts the peak from π. The factor of $\frac{1}{2}$ difference in d/δ_e for $b = 0$ and -1 is due, as discussed by Lampe and Platzman,[10] to the fact that in the thick-sample limit a symmetrically excited sample must be equivalent to a sample half as thick excited on only one side. For $\delta/\delta_e = 0.2$, curve A, the tail in the d/δ_e peak extends far enough to

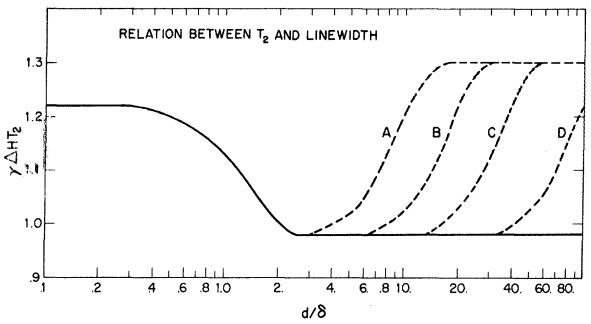

FIG. 6. Theoretical linewidth ΔH in units of $1/\gamma T_2$ vs d/δ for the derivative of the CESR power absorption. ΔH is defined by the insert to Fig. 4. Solid line: $\delta/\delta_e \ll 1$, $b = 0$ or -1; curve A: $\delta/\delta_e = 0.2$, $b = 0$; curve B: $\delta/\delta_e = 0.1$, $b = 0$; curve C: $\delta/\delta_e = 0.1$, $b = -1$; curve D: $\delta/\delta_e = 0.02$, $b = 0$.

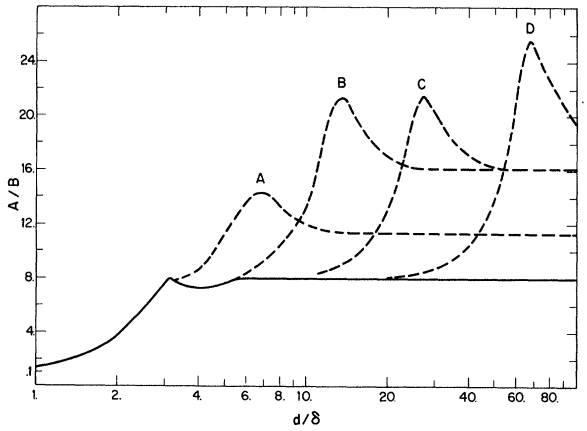

FIG. 7. Theoretical A/B vs d/δ for the derivative of the CESR power absorption. Solid line: $\delta/\delta_e \ll 1$, $b=0$ or -1; curve A: $\delta/\delta_e=0.2$, $b=0$; curve B: $\delta/\delta_e=0.1$, $b=0$; curve C: $\delta/\delta_e=0.1$, $b=-1$; curve D: $\delta/\delta_e=0.02$, $b=0$.

obscure the λ peak and the dirty film case is approached.

At the same time, as A/B rises to a peak, the line broadens again as shown by the dotted lines in Fig. 6. Note that the broadening is essentially complete by the time the peak in A/B is reached. There is only a very small g shift of the resonant field from the peak field.

D. Anomalous Skin Effect in Thick Films

When $d \gg \delta$, the surface impedance for spinless electrons is

$$Z_0 = (1+b^2)\,(1-i)\,\rho/\delta. \tag{15}$$

Taking this limit in Eq. (4) and retaining only the leading term in w, we find

$$Z = Z_0 + \frac{\pi\omega_0 T_2 \chi_0 d\delta^2}{\rho\delta_e^2}\,\frac{1}{(1+b^2)^2}\,\frac{Z_0^2}{w} \times[(1-b)^2\cot w - (1+b)^2\tan w]. \tag{16}$$

Lampe and Platzman[10] have shown that in this limit the only way that the anomalous skin effect (ASE) enters into Z is by changing Z_0. The variation of Z_0 has been calculated by Reuter and Sondheimer[16] for an infinite flat slab. They evaluated $X(\alpha)$ and $R(\alpha)$, where $Z_0 = R - iX$, $\alpha = 3l^2/2\delta^2$, and l is the mean free path, for two extreme surface conditions, diffuse ($p=0$) and specular ($p=1$) scattering of the electrons, and found that as α increases from 0, X/R starts to deviate from the classical value of 1 near $\alpha = 0.01$, and reaches an extreme value of $\sqrt{3}$ for $\alpha \gg 1$. The detailed variation of X/R with α depends on p, but the large α limit does not.

We can easily see the effect of this variation of Z_0 on the ESR line shape by taking the limit $d/\delta_e \ll 1$ in Eq. (16). This is the limit described classically by Eq. (12) with $\kappa=0$ and $\nu=-1$, which is a Lorentzian dispersion line shape with $A/B=8.0$. But now the ASE mixes the absorptive and dispersive signals so that

$$\frac{dP}{dH_0} = -\left(\frac{c}{4\pi}\right)^2 H_1^2\,\frac{2\pi\rho\omega_0 T_2\chi_0}{d}\,\frac{(1-b)^2}{(1+b^2)^2}\left(\frac{R}{R_0}\right)^2 \times\left[\kappa'\frac{d}{dx}\left(\frac{1}{1+x^2}\right)+\nu'\frac{d}{dx}\left(\frac{x}{1+x^2}\right)\right], \tag{17}$$

where

$$\kappa' = (X/R)^2 - 1, \tag{18}$$

$$\nu' = -2X/R, \tag{19}$$

and $R_0 = \rho/\delta$. As the ASE increases X/R from 1, some of the absorption signal is mixed in and A/B decreases instead of remaining constant. Figure 8 shows the theoretical variation of A/B with $\alpha^{1/6}$ for $p=0$ and 1 using Reuter and Sondheimer's variation of X/R with $\alpha^{1/6}$. Note that the large α limit of A/B is 3.6. For samples where d/δ_e is not extremely small, the line shape can be obtained from Eq. (16). If all the terms dropped by Lampe and Platzman are to be included, Eq. (4) can be used by multiplying Z by $Z_0'^2/Z_0^2$, where $Z_0' = R - iX$ and Z_0 is given by Eq. (15).

IV. COMPARISON WITH EXPERIMENT

A. Thin Samples above 120°K

Figure 9 compares the experimental line shape with the theory (circles). Apart from the x and y scale which were set by normalizing to the peak value and the half-signal linewidth, the only adjustable parameter is λ which was chosen for each curve to give the correct A/B ratio. The agreement is good even far out into the Lorentzian tails.

A more exacting test of the theory is to measure d and ρ so that λ can be calculated. Then there are

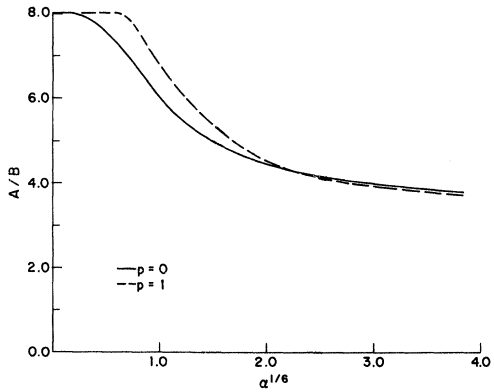

FIG. 8. Theoretical A/B vs $\alpha^{1/6}$ using Reuter and Sondheimer's values of X/R vs $\alpha^{1/6}$ for diffuse ($p=0$) and specular ($p=1$) reflection of the electrons at the surface. $\alpha = 3l^2/2\delta^2$.

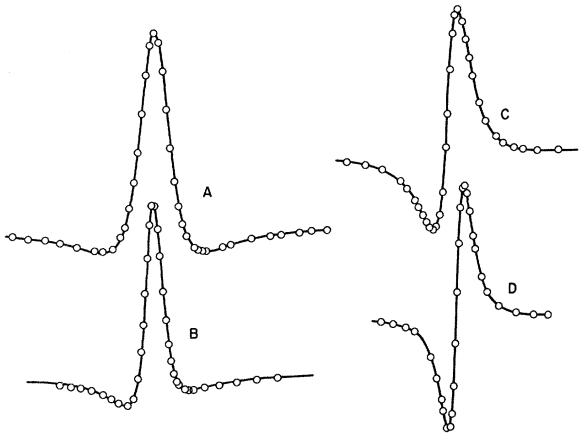

FIG. 9. Line shapes of the derivative of the CESR power absorption in lithium films. The solid lines are traces of experimental curves. Increasing H_0 is from right to left. The x and y scales of different line shapes are not related. The circles are theoretical points with $\delta/\delta_e \ll 1$. Curve A: $T = 276\,^\circ\mathrm{K}$, $\Delta H = 2.83$ G, $d/\delta = 3.14$; curve B: $T = 282\,^\circ\mathrm{K}$, $\Delta H = 3.20$ G, $d/\delta = 2.61$; curve C: $T = 287\,^\circ\mathrm{K}$, $\Delta H = 1.64$ G, $d/\delta = 1.28$; curve D: $T = 291\,^\circ\mathrm{K}$, $\Delta H = 2.71$ G, $d/\delta = 0.66$.

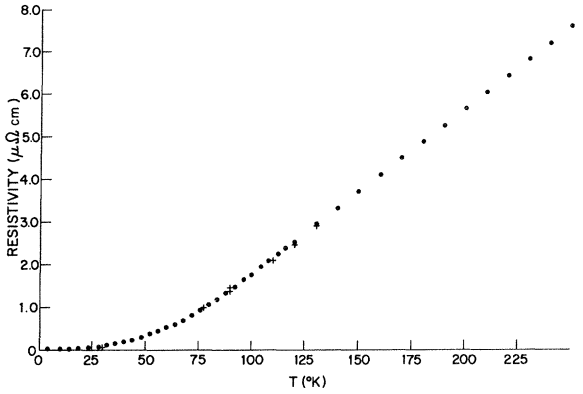

FIG. 10. Experimental resistivity vs temperature of a lithium film. The crosses are data taken by other workers on bulk lithium samples.

no adjustable parameters. Figure 10 shows typical dc resisitvity vs temperature data for a flat film prepared at the same time as a CESR sample. The resistance ratio $R(273)/R(4.2)$ is about 440, which is comparable to the ratio obtained on bulk samples of comparable purity. A further indication that the films can be regarded as bulk samples is provided by the crosses in Fig. 10 which are resistivity data reported by the other workers.[17,18] There is a slight disagreement in the shape of the resistivity curve below 30 °K which does not show up on the scale used. The resistivity is related to the measured resistance by $R = \rho L/Wd'$, where L and W are the easily measured length and width of the film and d' is the thickness. d' was obtained by fitting the resistance data above 120 °K with the straight line

$$R = \frac{L}{Wd'} \frac{d\rho}{dT} (T - T_c) \qquad (20)$$

with $d\rho/dT = 0.0385$ $\mu\Omega$ cm/°K as obtained by Dugdale *et al.*[17] on bulk lithium samples. The apparent intercept T_c, which depends on the impurity content, varied slightly from film to film but was typically 52 ± 1 °K.

The thickness d of the cylindrical film should be related to d' by $d'/d = \pi$. In practice, a much better fit to the theory is obtained if d is chosen to be about 10% larger than this value. This discrepancy would occur if the deposition rates on the two substrates were different, or if the microwave resistance differed from the dc.

Figure 11 compares the theoretical and experimental A/B ratios as a function of λ for a number of thin clean films. Since A/B is uniquely determined by λ, when $\delta \ll \delta_e$, all of these films fall on a universal curve regardless of the CESR linewidth or film thickness. d has been adjusted for each film to give the best fit near room temperature. Data below 120 °K has been eliminated to avoid departures from the classical skin effect. This region will be discussed later. The data shown in Fig. 11 is in good quantitative agreement with the theory. The estimated error, shown for one point, corresponds to an error in measuring B of only 2% of the peak-to-peak signal. The A/B ratio is extremely sensitive to the condition of the surface of the sample. Some of our earlier samples, prepared before the sample preparation techniques were under proper control,

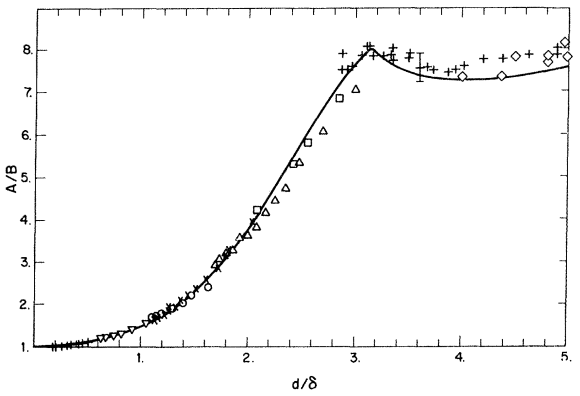

FIG. 11. A/B vs d/δ for the derivative of the CESR power absorption. The solid line is the theoretical curve for thin films with $\delta/\delta_e \ll 1$. The points are experimental data taken on lithium films between 300 and 120 °K. The following films were used: $d = 0.3$ μ, $\Delta H = 11.5$ G; $d = 1.0$ μ, $\Delta H = 5.4$ G; $d = 1.45$ μ, $\Delta H = 3.5$ G; $d = 1.8$ μ, $\Delta H = 0.56$ G; $d = 2.25$ μ, $\Delta H = 2.3$ G; $d = 2.55$ μ, $\Delta H = 2.3$ G; $d = 5.10$ μ, $\Delta H = 0.52$ G; $d = 7.62$ μ, $\Delta H = 1.6$ G.

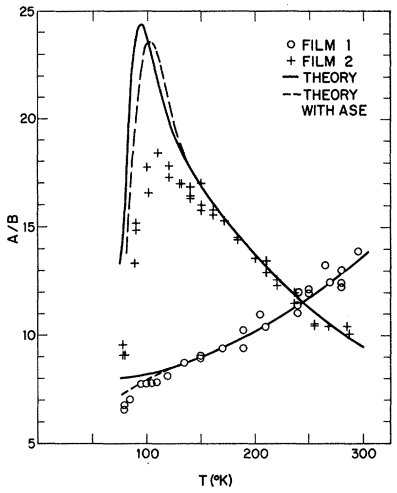

FIG. 12. Experimental A/B vs temperature for a clean and a dirty thick film. The thicknesses are about the same. The solid lines are theoretical fits. The dotted lines include theoretical corrections for the anomalous skin effect. Film 1: $d=17\ \mu$, δ/δ_e (300 °K) = 0.100, $\Delta H = 0.80$ G (clean); film 2: $d=21\ \mu$, δ/δ_e (300 °K) = 0.252, $\Delta H = 4.9$ G (dirty).

showed large deviations in the A/B ratio. Feher and Kip[2] have observed similar effects on A/B in very thick samples, which they attributed to surface roughness.

B. Thicker Films

It is somewhat difficult to compare the thick- or dirty-sample theory with experiment using films since for fairly pure metals δ/δ_e is small even at room temperature. Thus one must prepare a very thick and quite dirty film in order to get $d/\delta_e \approx 1$. Figure 12 compares the A/B ratios as a function of temperature for two films of roughly the same thickness. Film 1 was prepared in a clean system and had a room temperature linewidth of 0.8 G. Film 2 was dirtied by adding zinc[3] to the evaporation boat and had a linewidth of 4.9 G. The solid theoretical curves were obtained from Fig. 7 by taking into account the temperature variation of δ/δ_e, but ignoring the ASE. As the temperature decreases, λ increases as $\rho^{-1/2}$, while δ/δ_e decreases as ρ. Thus as λ changes one must move from curve to curve in Fig. 7. At room temperature for film 1, A/B lies part way up one of the peaks. As T is lowered, the peak moves out faster than λ, so that A/B moves back down the peak and approaches the plateau at 8.0. In film 2, A/B lies beyond the peak so that as T is lowered it rises, reaches the peak near 100 °K, and then drops in the same manner as film 1 did.

The theory was fitted to the experiment by choosing both δ/δ_e and λ. Film 2 was very sensitive to δ/δ_e in the high-temperature region. λ was chosen to make the peaks coincide. In film 2 the fit gave $d=21\ \mu$ which agreed with titration results within 2%. At 300 °K the fit requires $\delta/\delta_e = 0.252$. This ratio is easily calculated using the free-electron model where $D=\frac{1}{3}v_F^2\tau$. Using Fig. 6 to relate T_2 to ΔH, an effective mass of $1.4m$, and the experimental value of ρ, we find $\delta/\delta_e = 0.23$, in good agreement with the fitted value. The good quantitative agreement at high temperatures verifies the existence of the peaks predicted in Fig. 7. The disagreement at low temperature is due for the most part to the ASE. The dashed lines in Fig. 12 giving the theoretical correction for the ASE will be discussed in Sec. IV C.

Schultz, Shanabarger, and Paltzman[19] (SSP) have observed an anomaly in the A/B ratio of the transmission conduction spin resonance[20] (TESR) of dilute Cu:Mn alloys. The anomaly appears quite similar as a function of T to the peak in Fig. 12. It is interesting to inquire whether the anomaly has the same cause as the peaks we observe. The experimental configuration is somewhat different. In TESR field modulation is not used. Thus a given A/B ratio represents a different line shape for the two cases. A Lorentzian absorption curve has $A/B=1$ with modulation and ∞ without, while the dispersion curve has $A/B=8$ with modulation and 1 without. In addition, the phase of the TESR signal is set to give low- and high-field minima of the same amplitude; while in CESR the phase is set to give pure absorption if the sample were insulating. These differences will affect the details of any peak in A/B but not its presence or absence. The important difference is that TESR measures the transmitted rf field, not the absorbed power, that is, TESR measures b. We have taken[11] $b=0$. Thus the peak will not directly enter into the TESR signal. SSP have found that the transmitted rf field is proportional to $(\sinh k_2 d)^{-1}$. The manganese local moment affects the value of k_2 but not the functional form of the field. Numerical calculations show no peak when $d/\delta_e \approx \pi$.

C. Anomalous Skin Effect

In all films we found deviations from Dyson's theory below 120 °K due to the ASE. Films which satisfy the condition $\delta \ll d \ll \delta_e$ are particularly convenient to study the ASE since their CESR line shape should be independent of temperature except for ASE changes. Figure 13 gives the temperature dependence for two such films. The theoretical curves in the figure for diffuse and specular scattering are derived from Fig. 8 using values for $\alpha(T)$ calculated assuming the free-electron model, from the dc resistivity measured for each sample. The $p=1$ curve is in qualitative disagreement with the data, while the $p=0$ curve has the correct shape but is displaced to lower temperature than the data.[21]

This displacement is largely due to strains in the sample which arise since the film is constrained to a quartz substrate which has a very low thermal contraction. These strains are also responsible for the absence of the martensitic transformation which occurs in bulk lithium near 80 °K. Chambers[22] has shown that the surface impedance of an electropolished copper sample increases by an extreme amount when the surface is severely strained by mechanical polishing. He also showed that surface oxidation has a relatively minor effect. The shift in the data and the disagreement between the two samples may also be due to roughness and imperfections in the films due to variations in the cleanliness of the substrate, deposition rate, and the quality of the vacuum during evaporation. Visually the films appeared identical with bright mirror surfaces.

Deviations from the free-electron theory in lithium can also contribute to a shift in the direction observed. Since the discrepancy between the two films is almost comparable to the deviation from the theory, we are unable to extract any information on deviations from the free-electron theory. It would be worthwhile to improve the samples, since calculations by O'Keefe and Goddard[23] have predicted the appearance of gaps in the band structure of lithium within the first Brillouin zone.

At very low temperatures, when l becomes comparable to d, we expected deviations from the theory due to a breakdown of Reuther and Sondheimer's assumption of a semi-infinite sample, but no evidence is seen for this.

The technique is very sensitive to small deviations from the classical skin effect. At 100 °K the deviation of A/B from 8.0 is equal to the experimental error in measuring A/B. This deviation corresponds to a 2% change in X/R from its classical value. The sensitivity is even greater for the dirty film in Fig. 12. The dotted line shows the ASE correction to the classical A/B ratio. The disagreement of the data is again probably due to the imperfection of the surface, or perhaps is an impurity effect since the sample was intentionally dirtied with zinc. At low temperature A/B is much less sensitive to changes in X/R, as seen in Fig. 8.

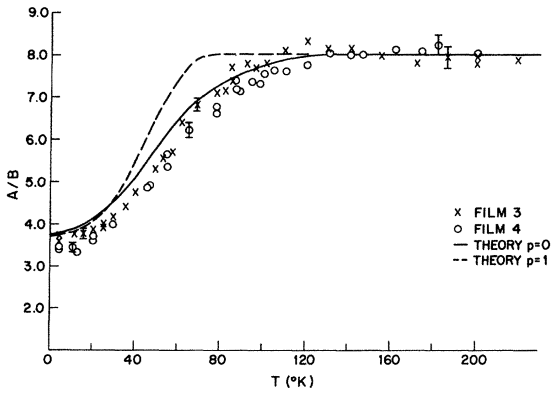

FIG. 13. Experimental A/B vs temperature for two clean lithium films of intermediate thickness. The theoretical curves are derived from Reuter and Sondheimer's calculation of the anomalous surface impedance using the experimental dc resistivity. Film 3: $d=6.0\ \mu$, $\Delta H=1.6$ G; film 4: $d=7.6\ \mu$, $\Delta H=1.4$ G.

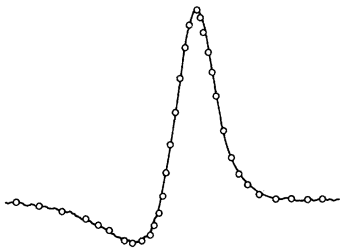

FIG. 14. Line shape of the derivative of the CESR power absorption in film 3 at 4.2 °K. Increasing H_0 is from right to left. The circles are theoretical points including corrections for the anomalous skin effect.

Finally we emphasize that the deviations we observe from Dyson's line shape corrected for the ASE are very small and the theory is entirely adequate for determining the true g value or spin-lattice relaxation time, even for relatively poor samples. Figure 14 compares the experimental line shape with the theory in the extreme ASE region. The reduced signal to noise is due to the very small skin depth.

V. CONCLUSION

We have shown that the use of a linear resonator is a simple technique for studying electron resonance in metals with moderately increased sensitivity. The small size and simple shape of the resonator should make the technique useful for studies of alloys and single crystals. The increased sensitivity should be useful in the study of surfaces. The intense rf field and the elimination of the closed cavity should be useful for ENDOR or double irradiation experiments.

We have applied the technique to verify Dyson's theory of the CESR line shape for a thin film of lithium in the intermediate region between extremely thin and thick samples. We find good qualitative agreement at high temperatures and also at low temperatures provided corrections are made for the anomalous skin effect. All deviations are consistent with strains or imperfections in the microwave surface of the sample. It is shown that the CESR asymmetry can be used to measure the microwave surface impedance in films of proper thickness and purity.

ACKNOWLEDGMENTS

We are grateful to Dr. D. Halford for sending us an unpublished description of his deformed linear

resonator which first aroused our interest in the technique, to Professor D. Langreth for finding an error in our calculation, to A. Gynn, M. Moskowitz, and S. Wolf for much useful advice on the art of making thin films, and to R. Longo for experimental assistance.

---

*Work supported in part by the National Science Foundation.

[1]F. Dyson, Phys. Rev. 98, 349 (1955).

[2]G. Feher and A. F. Kip, Phys. Rev. 98, 337 (1955).

[3]D. Halford (private communication); D. Halford and H. M. McConnell, J. Chem. Phys. 41, 898 (1964).

[4]J. C. Collingwood and J. W. White, J. Sci. Instr. 44, 509 (1967).

[5]A. B. Pippard, Proc. Roy. Soc. (London) A203, 98 (1950).

[6]Supplied by the Foote Mineral Co., Exton, Pa.

[7]J. I. Kaplan, Phys. Rev. 115, 575 (1959).

[8]H. C. Torrey, Phys. Rev. 104, 563 (1956).

[9]This is not true at very low temperatures in pure samples where an electron can complete a cyclotron orbit before scattering.

[10]M. Lampe and P. M. Platzman, Phys. Rev. 150, 340 (1966).

[11]We have solved for the correct value of b for a long cylindrical rod. Numerical calculations show that the difference from setting $b=0$ is negligible.

[12]The usual definition is the ratio of the low-field peak to the high-field peak. There is a difference only for $\pi < \lambda < 2\pi$.

[13]We used the Rutgers Bubble Chamber Group's PDP-6 computer (supported by the National Science Foundation).

[14]H. Kodera [J. Phys. Soc. Japan 28, 89 (1970)] has recently done similar calculations for a degenerate semiconductor where $\delta_e/\delta \ll 1$.

[15]If the usual definition of A/B (Ref. 12) had been used in Fig. 3, it would have shown the same peaked behavior shown in Fig. 6.

[16]G. E. H. Reuter and E. H. Sondheimer, Proc. Roy. Soc. (London) A195, 336 (1948).

[17]J. S. Dugdale, D. Gugan, and K. Okumura, Proc. Roy. Soc. (London) A263, 407 (1961).

[18]D. K. C. MacDonald, G. K. White, and S. B. Woods, Proc. Roy. Soc. (London) A235, 358 (1956).

[19]S. Schultz, M. R. Shanabarger, and P. M. Platzman, Phys. Rev. Letters 19, 719 (1967).

[20]R. B. Lewis and T. R. Carver, Phys. Rev. Letters 12, 693 (1964); N. S. VanderVen and R. T. Schumacher, *ibid.* 12, 695 (1964).

[21]The usual criterion given for ASE to occur is $\delta \approx l$, which occurs at 50 °K but note that effects are seen as high as 120 °K.

[22]R. G. Chambers, Proc. Roy. Soc. (London) A215, 481 (1952).

[23]P. M. O'Keefe and W. A. Goddard III, Bull. Am. Phys. Soc. 14, 1164 (1969).

PHYSICAL REVIEW B VOLUME 3, NUMBER 3 1 FEBRUARY 1971

Effect of Brownian Motion on the Mössbauer Line Shape

V. G. Bhide, R. Sundaram, and H. C. Bhasin
National Physical Laboratory, New Delhi, India

and

T. Bonchev*
Sofia University, Sofia, Bulgaria

(Received 4 May 1970)

A general theoretical expression for the resonance-absorption cross section of γ rays by particles in liquids is worked out. The treatment takes into account the general solution of the Langevin equation, thereby revealing the important role played by the characteristic time of the liquid. While the line shape predicted by Singwi and Sjölander takes care of atomic motion, it is inadequate for the motion of particles in liquids. When composite particles are used, the nuclear lifetimes of the Mössbauer isotopes may be compared with the characteristic time of the liquid. It is shown that, under certain conditions, narrowing of the Singwi-Sjölander line can be considerable.

I. INTRODUCTION

It has been long recognized that the resonance absorption of γ rays, otherwise known as the Mössbauer technique, could be used to investigate the nature of diffusive motion in liquids. Singwi and Sjölander,[1] using the space-time correlation function of van Hove, have derived an expression for the resonance-absorption cross section. They have predicted a diffusive broadening of the resonance line proportional to the diffusion coefficient of the liquid and the square of the γ-ray energy.

In this laboratory, some experiments have been conducted using a composite particle containing two Mössbauer isotopes. An $FeSnO_3$ suspension in machine oil was used, and the line broadenings of ^{119}Sn and ^{57}Fe were compared. The ratio should have been the ratio of the squares of the two γ-ray